M.J. Kadhim
Department of Production Engineering and Metallurgy, University of Technology Baghdad, Iraq

M.H. Hafiz
College of Engineering, Al-Iraqi University, Baghdad, Iraq

M.A. Ali bash
Department of Production Engineering and Metallurgy, University of Technology Baghdad, Iraq
soukaena.hassan@yahoo.com

Microstructure and Phases Analysis for Advanced Plasma Sprayed Zirconia-Ceria-Yttria Thermal Barrier Coating

Abstract-*Thoroughly qualitative and quantitative topography, microstructure, splats formation and phases evaluation were made to understand carefully the behavior of plasma sprayed zirconia-ceria-yttria coatings processed under near optimum processing conditions. The study is focused on how to design and select the given property to predict the reliable data of plasma sprayed zirconia-20 wt% CeO_2-3.6 wt% Y_2O_3. The processing and plasma spraying parameters were designed carefully to give a reliable clear evaluation of the microstructure. The results showed a heterogeneous microstructure in which melted, semimelted and unmelted particles were existed. The phases formed are consisted of nontranformable tetragonal phase (t') with small amount (less than 2 mole%) of monoclinic phase (m). The electron probe microanalysis (EPMA) suggests the intimate mixing between the binary systems of zirconia-ceria and zirconia-yttria during spraying. The Image J technique, SEM, EPMA, EDS and XRD/step scan XRD were used collectively to build up a clear picture on the solidification mechanism of the new plasma sprayed coating system.*

Keywords- *Plasma sprayed ceramic; Zirconia-ceria-yttria; Advanced engines; Electron probe microanalysis*

How to cite this article: M.J. Kadhim, M.H. Hafiz and M.A. Ali bash, "Microstructure and phases analysis for advanced plasma sprayed zirconia-ceria-yttria thermal barrier coating" *Engineering and Technology Journal*, Vol. 35, Part A, No. 10, pp. 1025-1033, 2017

1.Introduction

These days, zirconia based thermal barrier coatings (TBCs) are considered the most important ceramic systems to overlay excellent hot corrosion resistance and thermal insulation for many advanced superalloy engines. However, there are many discrepancy regarding the phases, hardness, fracture toughness and physical properties after plasma spraying. Over the past sixty years the developments of high temperature ceramic oxides have been taken great attentions for utility, diesel and gas turbine engines applications. This has led to develop many superalloys, bond coats, zirconia based thermal plasma sprayed coatings and many thermal barrier coatings (TBCs) [1,2]. Components of such engines should have a wide spectrum of combined properties like high strength, resistance towards oxidation, creep, fatigue, thermal stability, thermal conductivity, erosion, hot corrosion, in addition to good thermal stability and thermal conductivity at high temperatures [3,4]. It is very important to any one dealing with zirconia based ceramic thermal barrier coatings stabilized with many oxides such as yttria, ceria, scandia and others to understand carefully the existed phases and topography of plasma sprayed coatings [5,6]. It is important to report that yttria partially stabilized zirconias (YPSZs) have been considered the important thermal barrier coating systems having nontransformable tetragonal phase (t') [7]. Stabilizing zirconia with other oxides such as ceria may produce other metastable phases [8]. They have very high melting points, chemical inertness, oxidation resistance and high fracture toughness [9-11]. The state-of-the art of plasma sprayed coatings used at high temperature application show that zirconia-yttria and zirconia-ceria are the most dominant [12].Plasma sprayed thermal barrier coatings systems are vital to be used in many modern ground engines, gas turbine engines and diesel engines [13]. The main reasons are to lower the substrate superalloy temperature and consequently increase the efficiency. These days both land based and aero-jet propulsion engines enjoy the advantages of the plasma sprayed technology. The most important advantages recognized successfully are reducing the fuel consumption with higher power thrust and lower nitrogen mono-oxide (NOx) (NO and NO_2) [14]. The lower corrosion resistance at high temperatures and phase transformation occurs above 1200^{o}C limits the upper operating temperature of yttria stabilized zirconia [15]. It was reported that ceria

Copyright © 2017 by UOT, IRAQ

stabilized zirconia system have a superior thermal shock resistance to those based on the yttria stabilized zirconia systems [16]. Therefore, addition of ceria to yttria partially stabilized zirconia plasma sprayed coatings may improve the thermal cyclic life and corrosion resistance.The most ceramic coatings are produced only by either electron beam physical vapor deposition (EB-PVD) or thermal plasma spraying (TPS) [17,18]. There were also some attempts into development new techniques and ceramics to cope with the concepts of TBCs [19,20]. Till now, the most important advanced components such as valves, nozzle, turbine blades and combustor are coated using thermal plasma spraying. This technique is much complex than EB-PVD. It controls by several dependent, independent and dependent-independent variables. Therefore, careful selection for the processing sheet for thermal plasma spraying is required. Different features such as porosity, cracks, melted particles, semi-melted particles, un-melted particles and finishing of the coatings may be produced. The point views concern of metallurgists and ceramists are related in-depth to develop and understand how to enhance the TBCs [21,22]. Detailed investigations and analysis of literatures highlight many important points till require to resolve [23-26]. The most important is processing of plasma sprayed thermal barrier coatings ceria stabilized zirconia need to be investigated [27-30]. It appears that any design improvement of the constituents of zirconia-ceria-yttria plasma sprayed coating which eliminating the porosity and cracking may enhance the performance of TBCs. This will be only successful if the other requirements of the system will not be altered. The aim of this paper is to investigate and develop promising plasma sprayed thermal barrier coating based on ternary system zirconia-20 wt% CeO_2-3.6 wt% Y_2O_3.

2.Experimental procedures

The substrate for plasma sprayed thermal barrier coating system used in this study is the standard reliable Ni- based superalloy substrate TM IN-738 LC. The substrate samples used were discs with 3 mm thickness and 25 mm diameter. The samples were firstly cleaned with diluted HCl with water, alcohol and acetone. The samples were then ground with 120 SiC emery paper and cleaned again in alcohol. In order to increase the bonding between the substrate and bond coat layer, the samples were alumina blasted and cleaned again in alcohol (Table 1). Thermal barrier coating system investigated in this study is based on bond coat powder type Amdry 963 (Ni24.5Ni10Al0.4Y) used to produce the inner bond coat and the upper ceramic coating is based on a mixture of Sulzer Metco 205NS (ZrO_2-25 wt% CeO_2-2.5 wt% Y_2O_3) and Sulzer Metco 204NS-G (ZrO_2- 8 wt% Y_2O_3) powders. The weight ratio of these ceramic powders (g) is 80% Sulzer Metco 205NS and 20% Sulzer Metco 204NS-G. This ratio of the mixed ceramic coat investigated is a new system based on ZrO_2-20 wt% CeO_2-3.6 wt% Y_2O_3. The detail analysis of the mixed powders was published other else [31]. The bond coat is a typical standard bond coat used for thermal barrier coating. The nominal size distribution ranges for bond coat (Amdry 963), Sulzer Metco 204NS-G and Sulzer Metco 205NS ceramic powders are -90 +45, -125 +11 and -125 +11 μm respectively. Atmospheric plasma spraying coating unit manufactured by Metco INC, Westury, L.I.N.Y company (Fig. 1) was used to plasma sprayed both the bond coat of Amdray 963 and the mixed Sulzer Metco 205NS and Sulzer Metco 204NS-G (80 wt% and 20 wt%) coatings respectively onto the IN-378 LC superalloy. The plasma gun type 3MB manufactured by Metco INC, Westbury, L.I.N.Y. The processing sheet for alumina blasted and plasma spraying coatings were designed completely by the authors. Many initial experiments were made to select the reliable spraying conditions. The discs of IN-738 LC superalloy samples were shot alumina blasted just before the spraying process. The plasma sprayed features were determined from thoroughly analysis of the upper surface plan views without grinding or polishing using firstly optical microscopy (OM) and secondly scanning electron microscopy (SEM). Samples were then ground genteelly from the plan view using 1200 SiC emery paper and polished using 0.05 μm γ-Al_2O_3 to determine the microhardness. Microhardness measurements were also performed from transverse sections. The transverse sections were cold mounted and then ground using a special jig to maintain the alignment of the two perpendicular surfaces. The surfaces were ground using 120 and 600 grade SiC emery papers respectively. The samples then polished with 3 μm diamond paste and finally with 0.05 μm γ-Al_2O_3. The polished samples were etched selectively for both substrate and bond coat using 15 cc HCl+ 10cc Glycerol + 5cc HNO_3 solution. Different types of scanning electron microscopies (SEM) namely, Cambridge- S360, Tescan VEGA3LM and Tescan VEGA 3SB were used to analyze the upper plan views and transverse sections. The quantitative determinations of energy dispersive spectroscopy (EDS) were carried out using electron probe microanalysis (EPMA). Carbon evaporation and gold sputtering were used to deposit thin film layers on the ceramic surfaces to

enhance the electrical conductivity of the nonconductive ceramic coatings.

X-ray studies were employed to determine the qualitative and quantitative phases using different X-ray diffractometers. Shimadzu AA 1234 system was used employing nickel-filtered copper Kα radiation consisting of Kα1 and Kα1 with radiation wave length 0.154056 nm and 0.154439 nm respectively. All the X-ray diffraction tests were monitored at 2θ angle 20 up to 80°. The samples were scanned at different speeds from 1 to 5° 2θ/min. The samples were scanned with 2θ of 0.01° interval at a count time of 1 sec/step. The phases and their reflecting planes were identified by applying the experience in field of zirconia, X-ray diffraction analysis procedures, previous literatures and the ICDD (JCPDS) standard data.

The quantitatively analysis of the phases were determined based on the literature which cover the ranges of 27.5 to 32.5° and 72-75.5° 2θ respectively. Planes of {111} for 2θ 27.5 to 32.5° and {400} for 2θ 72-75.5° with the position of 2θ and their corresponding relative intensities (area under the curve) using Adams and Cox [32], Miller et al [33] and Iwamoto and Umesaki [34] based on Porter and Heuer [35] analysis were used to determine the volume or molar fraction of the phases. These equations are:

$$V_m = 1.603\, I(\bar{1}11)m / [1.603\, I(\bar{1}11)m + I(111)c + I(\bar{1}11)t + I(111)t'] \quad \text{…….(ref.32)}$$

$$X_m = 0.82\, [I(\bar{1}11)m + I(\bar{1}11)m] / 0.82\, [I(\bar{1}11)m + I(\bar{1}11)m + I(111)c + I(111)\bar{t}] \quad \text{…….. (ref. 33)}$$

$$X_{t^-} = (1 - X_m)\, 1.14\, [I(400)\bar{t} + I(004)\bar{t} / 1.14[I(400)\bar{t} + I(400)c + I(004)\bar{t}] \quad \text{……..(ref. 34)}$$

$$X_c = 1 - (X_m + X_{t^-})$$

$$\bar{t} = t + t'$$

where V_m is the volume% of monoclinic phase, X_m is the mole% of monoclinic phase, X_c is the mole% of cubic phase, X_{t^-} is the total mole% of transformable (t) and nontransformable (t') tetragonal phases, I (xxx)m, I (xxx)c and I (xxx)t are the corresponding intensities of the given peaks. It should be mentioned that the volume% is approximately equal to mole % [33].

Table 1: Processing sheet of bond coat and Sulzer Metco 205NS zirconia based plasma sprayed coatings.

Processing sheet of shot blasted		
Substrate	Ground SiC Inconel IN- 738 LC superalloy	
Blast material	alumina	
Blast Pressure	4 bar	
Blast distance	150-200 mm	
Processing sheet of plasma spraying of thermal barrier coatings		
	Bond coat	Ceramic coat
Primary gas	Ar	Ar
Pressure, bar	6.89	6.89
Flow rate, SLPM	39.95	53.25
Secondary gas	H_2	H_2
Pressure , bar	3.44	3.44
Flow rate, SLPM	6.11	7.52
Current, A , Ampere	450	525
Voltage (V), Volt	50	55
Spray distance, mm	120	70
Angle, %	90°	90°
Carrier	Ar	Ar
Flowrate , SLPM	13.16	17.39
Powder feed rate, g/min	45	35

Figure 1: Plasma sprayed unit used in this investigation.

3.Results and discussions

In this work, the general features of as-sprayed CYSZ coating were thoroughly evaluated for the features of topography, roughness, microstructure, phases, defects, chemical analysis and bonding between layers of the coating system. Fig. 2 shows the typical OM and SEM of upper surface plan views of as-prepared plasma sprayed coating

zirconia-ceria-yttria without grinding and polishing. It revealed clearly the non-uniform and uneven distribution of open porosity, some unmelted particles, semi melted particles, primary and secondary cracks and rough appearance. More details regarding the topography of the plasma sprayed coating formation can be found in the work of one of the authors [30]. Higher magnification of the upper surface plan views show the presence of overlapped microstructure of solidified particles. These were confirmed from SEM and Image J.

The microstructure is composed of two different structures revealed from SEM photography. The first one was with high volume fraction of complete melting of the sprayed powder. The second structure was with relatively small volume fraction consisted of semi melted and unmelted particles. This is related partially to the wide range of particles distribution. The average high roughness of plasma sprayed coating (6.2 ± 1 μm) is believed to be related highly to the partially or unmelted sprayed particles. The presence of these particles are highly due to reduce the flatted of solidified particles compared with fully melted particles. Part of this roughness is also due to the shadow mechanism of plasma sprayed phenomena.

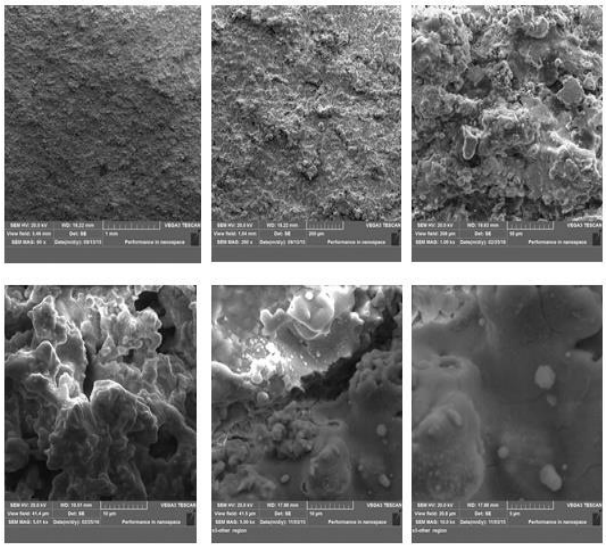

Figure 2: Typical SEM photographs of upper surface plan views of plasma sprayed zirconia-20 wt% ceria- 3.6 wt% yttria (CYSZ) at different magnifications showing the heterogeneous distribution of melted splats, semimelted and unmelted particles.

The general appearance of microstructure also showed the presence of microcracks which is formed due to the rapid solidification mechanism of sprayed particles; it generates thermal stresses or quenching stresses [36]. The volume fraction of open voids and porosity determined from upper surface plan view using Image J is approximately 14.9 ± 0.9% (Fig. 3). Detailed investigations of the upper surface plans views and as well as the transverse sections of plasma sprayed samples revealed that the structure is a typical of splat formation with good bonding between the ceramic and bond coatings (Fig. 4). Higher magnification 4intrasplats structure resulted from the detail of the splats. They consist of fine cell structures observed mostly from upper surface plan views. The microstructure was revealed without any chemical etching due to severe thermal etching associated with rapid solidification.

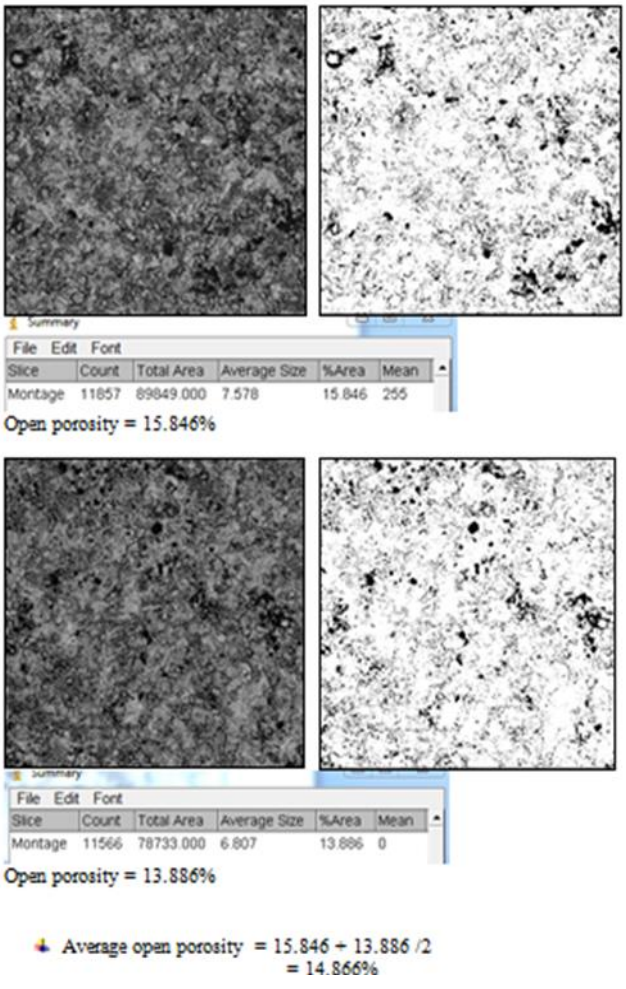

Figure3: Appearance of SEM micrographs of upper surface as-sprayed plan view and Image J showing the average open porosity.

This microstructure was considered as metastable structure due to the prevention of achieving the equilibrium phases. It is believed that the formation of metastable structure is mostly resulted in anisotropic coating with different properties in the z direction perpendicular to the coating thickness and to the x and y planes parallel to the coating thickness.

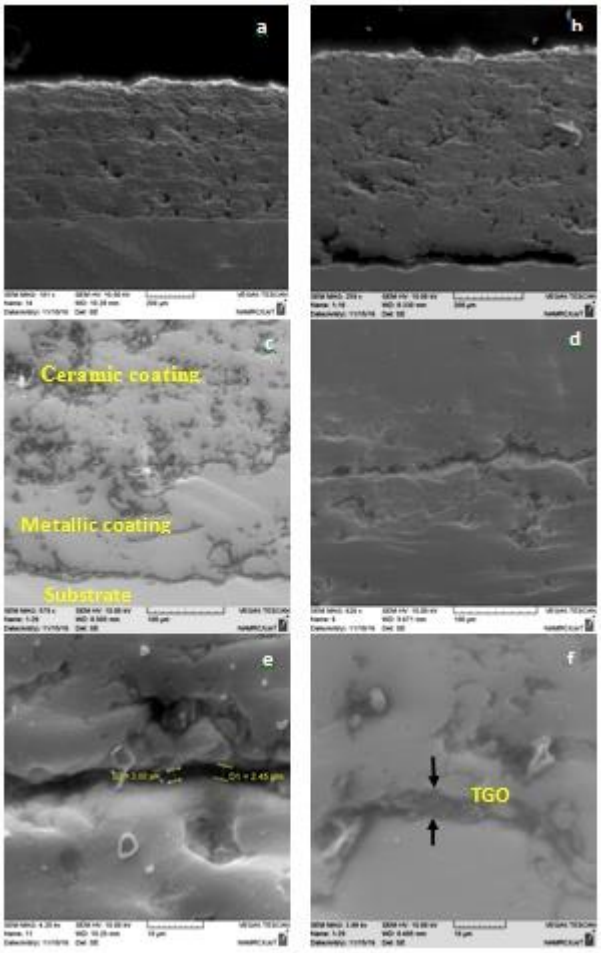

Figure 4: Typical SEM photographs of transverse sections of plasma sprayed (CYSZ); (a) and (b), (c) and (d) higher magnification of interfaces between coatings, (e) and (f) thermally grown oxide layers.

Electron probe microanalysis (EPMA) and area digimapping showed the relatively acceptable homogeneity of plasma sprayed coatings resulted from both the high homogeneity of staring powder and the rapid solidification (Fig. 5). Despite this chemical homogeneity, some oxide inclusions were also observed. These oxide inclusions in plasma sprayed of bond coat are known as stringers. They appeared as black areas (Fig. 4).

The typical transverse sections shown in Fig. 4 reveal the different components of the plasma sprayed thermal barrier coating (substrate, bond coat, thermally grown oxide and plasma sprayed coating). It shows the Ni-24.5 wt% Cr-10 wt% Al-0.4 wt% Y bond coat near to the substrate and the ceria-yttria stabilized zirconia coat adjusted to the bond coat. The thicknesses of ceramic top coat and bond coat are approximately 400 ± 25 μm and 90 ± 15 μm respectively. Higher magnification observations to the interface between bond coat/ceramic showed the presence of fine layer of approximately less than 2 μm thickness namely thermally grown oxide (TGO) (Fig. 4). Detailed examinations of the interface between the components of thermal barrier coating system studied revealed that the bonding between the bond/ceramic coatings is better than that between IN-738 LC superalloy/bond coatings.

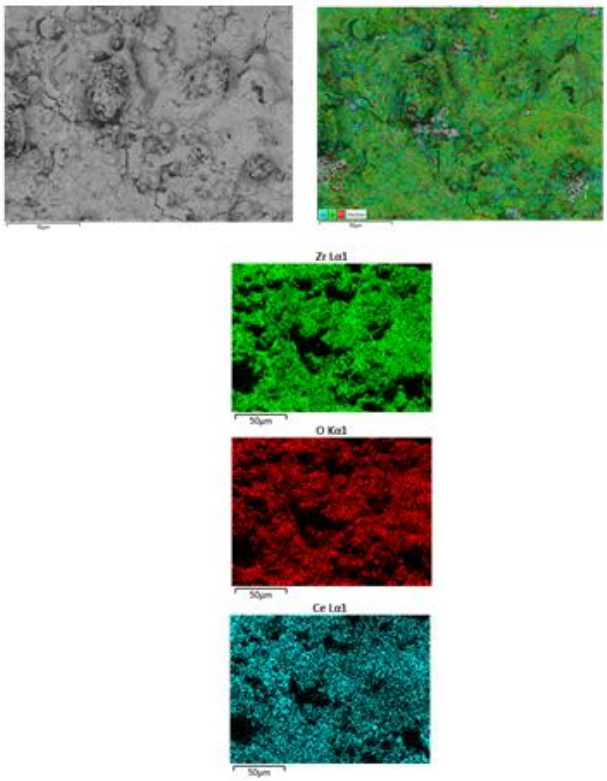

Figure 5: SEM micrograph and elemental X-ray mapping of the upper surface plan view of as-sprayed CYSZ.

The microstructure of plasma sprayed ceramic coating elucidated the mechanism of solidification is taken place by relatively low velocities of accelerated melted powders inside the plasma. The impingement of molten particles upon the superalloy substrate produces rapid solidification lamella. The lamella structure was found to be due to relatively incomplete flattened of the most particles to form the "splats" associated with semiautomatic plasma torch and larger particles size. The volume fraction of closed voids and porosity from the transverse section of the ceramic coat is relatively lower than the open void and porosity (approximately 11 ± 0.3%) (Fig. 6).

The porosity was consisted mostly with separate closed one with some interconnected porosity. The reason for high volume fraction of porosity is due to non-complete perpendicular between the solidified splats and substrate and to the mechanism of solidification particle by particle. This will generate relatively higher inter-lamellar pores.

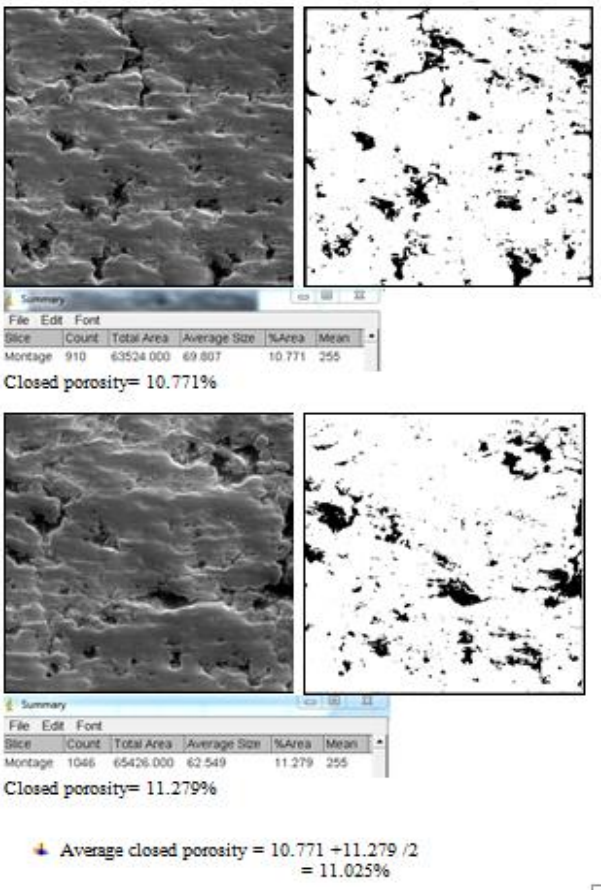

Figure 6: Appearance of SEM micrographs of as-sprayed transverse sections and Image J showing the average closed porosity.

The rapid solidification process of the splats is also played a role in the porosity formation especially for fine pores. The amount of porosity in the bond coat is much less than the ceramic coating (approximately less than 2%). Investigation of the plasma sprayed fracture surface reveals the microstructure is bimodal which consisted of columnar grains and nanosized unmelted powders (Fig. 7).The typical X-ray diffraction patterns of yttria partially stabilized zirconia mixed powder of Sulzer Metco 204NS-G and Sulzer Metco 205NS showed the presence of transformable tetragonal (t) phase with small amounts of monoclinic (m) phase; no cubic (c) was observed. The volume fractions of these phases are listed in Table 2. The plasma sprayed coating based on the power mixture has mainly nontransferable (t') phase as illustrated from high angle range (72-75.5º) with small amount of monoclinic (m) phase (less than 2 mole%) as illustrated from low angle range (27.5-32.5º) (Fig. 8 and Table 2). The high angle range peaks are fitted with (400) t' phase not with tetragonal (t) phase. Examination of the peaks profile at this range showed the absence of cubic phase as well as the t phase [37]. It can be seen clearly from X-ray diffraction data of the starting mixed powder [30] and plasma sprayed coatings the different phases formed in both the mixed powder and the plasma sprayed coating. The phases of the starting powder (t and m phases) have been changed entirely after plasma spraying. This is due to the nontransformable phase transformation associated with rapid solidification of plasma spraying.

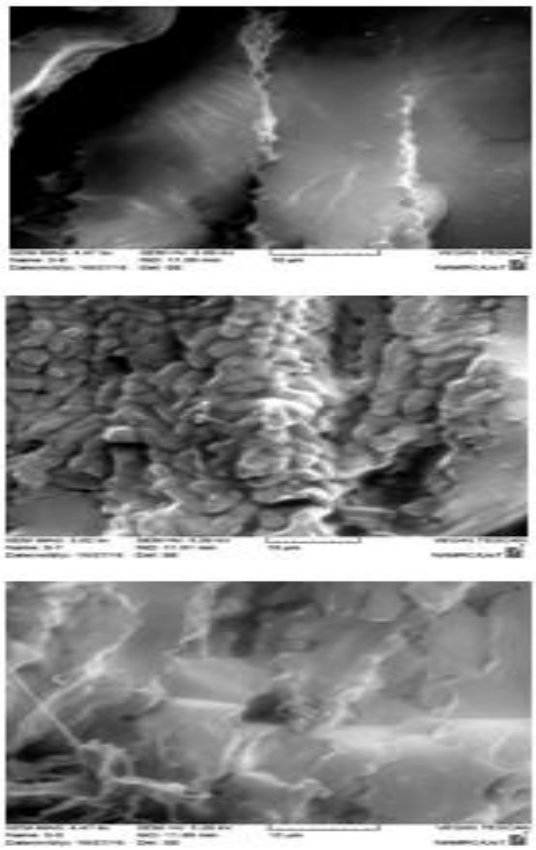

Figure 7: SEM micrographs of fracture cross section of as-sprayed CYSZ showing the bimodal structure.

The powder contains mixture of transformable tetragonal phase (t) and some monoclinic (m) and without noticeable amount of cubic (c) phases. The volume fractions of these phases are 82 ± 2 mole % and 18 ± 2 mole% respectively (Table 2). These volume fractions are determined from the low angle diffraction pattern in the range of 2θ (27.5-32°) and high angle diffraction pattern in the range of 2θ (72-75.5°) using the calculations mentioned in the literature [33]. The low angle range determined the mole% for m phase from m peaks of ($\bar{1}$11) and (111), while the high angle range determine the mole% of t phase from tetragonal peaks of (004) and (400) (Table 2). It should be very important to mention that the accuracy of determination of mole% of t or t' phases within ± 5% error. This is because the overlapped of t or t' peaks with cubic peak at relatively small 2θ value which gives relatively difficulty in resolving the peaks. Approximate fitting to Gaussian distribution was used to overcome these overlapped [37].

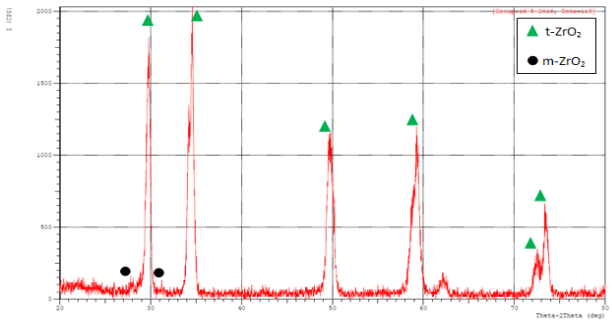

Figure 8: XRD pattern of the plasma sprayed CYSZ showing the presence of t phase with very small amount of m phase.

Table 2: Typical mole % of m, t, c and t' for mixed powder, plasma sprayed coatings and laser sealed coatings.

Ceramic type	Mole % m	Mole % c	Mole % t	Mole % t'
Mixed powder	18 ± 2	nil	82 ± 2	nil
Plasma sprayed coatings	1 ± 0.3	nil	nil	99

Careful examination of low 2θ range (27.5-32.5°) for plasma sprayed coatings shows the presence of small intensity peaks of m phase with strong peak of t or t'. This reduction in density of m is corresponding to lower mole%. Detailed investigation of higher range of 2θ (72-75.5°) demonstrated the presence of only two peaks of t or t' without the intermediate peak of c phase. Reference to detail X-ray diffraction literature, the position of t and t' phases are confirmed these peaks to t' phase rather than t phase. The t' phase in the plasma sprayed coating is distinguished with t phase in the starting powder according to the results of Mohammed Jasim [36] and Miller [33]. Therefore, mainly nontransformable tetragonal phase (t') with small amount of monoclinic phase (less than 2 mole%) and without any cubic phase were observed in the as-sprayed coating (Fig. 9). The absence of a high volume fraction of m phase in plasma sprayed coatings suggests clearly the high homogeneity of the phases in the sprayed coatings regardless the particles size distribution. Careful examinations of the intensity of the (200) did not showed the relative of higher density of this peak which clearly suggested the absence of any preferred orientation; the direction of (200) peak is [100] direction. The measured lattice parameters of t and t' with the c/a ration are listed in Table 3. It can be seen clearly the c/a ratio of t' phase approaches to a unity due to decrease of c value from 0.5234 nm for t phase to 0.5212 nm for t' (Table 3). Detailed analysis of lattice parameters measured showed that there was some discrepancy with the standard JCPDS files, ICDD files and literature [36]. This is because the lattice parameters are highly affected by the type and percentage of stabilizing as well as the processing.

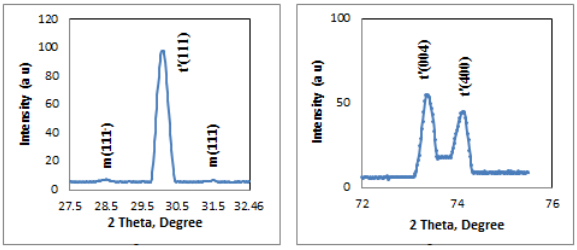

Figure 9: XRD of Plasm sprayed CYSZ.

Table 3: Crystal parameters data for the monoclinic (m), transformable tetragonal (t) and nontransformable tetragonal (t')

Value	Powder (ref. 31)	Plasma sprayed coating
a, nm	0.5132	0.5162
c, nm	0.5234	0.5212
c/a ratio	1.0198	1.0097
I_t or $I_{t'}(004)/(400)$	04-0.6	0.4-0.6
Δ2θ{400} t	1.2-1.3	-
Δ2θ{400} t'	0.4-0.6	0.7-0.8
$I_m(ī11)/ I_m(111)$	0.9	1.2

EPMA of plasma sprayed coatings suggested the relatively homogenous chemical distribution of ceria and yttria in the ternary solid solution of zirconia based t' phase (Fig. 10). This may be explained to the reason that both powders of the mixture (YPSZ and CSZ) have nearly similar small particle sizes and density. These will lead to be having same mass velocity when reaching and impingement on the substrate during spraying. Therefore, the trajectories inside the plasma powder travelling are nearly the same. This is resulted in the same thermal histories and producing relatively uniform chemical homogeneity. The relatively high chemical homogeneity of plasma sprayed coatings is believed to be due to producing ternary solid solution of particles (t' phase). This will take place due to the reaction of different particles during travelling of the plasma sprayed melted powders from the torch until reaching the substrate. Electron probe microanalysis (EPMA) was highly suggested this observation. This explanation is very important to analysis of phases present in plasma sprayed coatings of premixed powder.

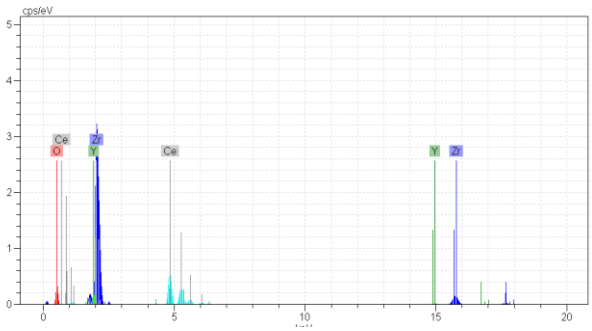

Figure 10: Typical EDS analysis of plasma sprayed coating showing the elements.

The relatively lower amount of m phase in the plasma sprayed coatings is related directly to high cooling rate of approximately 10^5-10^7 ^{o}C/s [36,38]. The formation of t' in plasma sprayed coatings is related directly to the rapid cooling rate associated with rapid solidification and temperature gradients [36,38]. This was suggested from EPMA (Fig. 10). It is clear evident that the cooling rate during plasma spraying was highly sufficient to prevent the equilibrium transformation of t to m phase due to formation of t' phase. The absence of any t phase is related directly to the small amount of un-melted particles in the coating. On the other hand, the absence of m phase presents highly in the powder is due to completely transforms of m phase upon melting of powder to t' and consequently solidified as t' phase.

4. Conclusions

1- The processing sheet of thermal plasma spraying coating is vital to be selected carefully for the thermal barrier coatings to produce ternary system of zirconia solid solution containing ceria and yttria from the binary zirconia-ceria and zirconia-yttria.
2- The general appearance of surface topography and transverse section of plasma sprayed coating was consisted of semi-melted and completely melted particles; with small amount of non-melted particles.
3- The plasma sprayed coating contains relatively considerable volume fraction of porosity but with good cohesion which is favorable for extra surfacing.
4- The microstructure of the plasma sprayed coating has intrasplat structures associated with high cooling rates which generate network cracking.
5- Addition of yttria to ceria stabilized zirconia does not affect the phases of plasma sprayed coating. The dominant phase is t' with small amount of monoclinic phase.
6- The plasma sprayed coatings have relatively high homogeneity of chemical composition due to intimate reaction during spraying flying and rapid solidification process.
7- The bonding between the ceramic coating/bonding coatings is much better than bond coating/substrate.

References

[1] P. Duwez, F. Odell, Phase relationships in the system zirconia-yttria, J. of the American Ceramic Society, 33(1950)274-283.
[2] H. Blairbarlett, R.R. Thomas Jr, A study of the mineralogical and physical characteristics of two lithia-zirconia bodies, J. of the American Ceramic Society, 17(1934)17-20.
[3] A.R. Miller, Thermal barrier coatings for aircraft engines: History and directions. J. of Thermal Spray Technology, 6(1997)35-42.
[4] J. Kaspar, O. Ambroz, Plasma spray coatings as thermal barriers based on zirconium oxide with yittrium oxide. In the 1st Plasma-technik symposium, Vol. 2, (Lucerne Switzerland, 18–20 May 1988), ed. H. Eschnauer, P. Huber, Andrew R. Nicoll and S. Sandmeier. Plasma-Technik AG, Wohlen, Switzerland, 1988, pp. 155-166.
[5] C.S. Ramachandran, V. Balasubramanian, P.V. Ananthapadmanabhan, V. Viswabaskaran, Influence of the intermixed interfacial layers on the thermal cycling behavior of atmospheric plasma sprayed lanthanum zirconate based coatings, Ceramics International 38(2012)4081-4096.
[6] R. Ahmadi-Pidani, R. Shoja-Razavi, R. Mozafarinia, H. Jamali, Improving the thermal shock resistance of plasma sprayed CYSZ thermal barrier coatings by laser surface modification. Optics and Lasers in Engineering, 50(2012)780-786.
[7] G. H. Scott, Phases relationships in the zirconia-yttria system, J. of Materials Science, 10(1975)1527-1535.
[8] F. Zhang, C. Chen, J. C. Hanson, R. D. Robinson, I. P. Herman, S.W. Chan, Phases in ceria-zirconia binary oxide (1-x)CeO_2-xZrO_2 nanoparticles: The effect of particle size, J. of the American Ceramic Society, 89(2006)1028-1036.
[9] G. Sattonnay, S. Moll, V. Desbrosses, V. Menvie Bekale, C. Legros, L. Thomé, I. Monnet, Mechanical properties of fluorite-related oxides subjected to swift ion irradiation: Pyrochlore and zirconia, Nuclear Instruments and Methods in Physics Research B, 268(2010)3040-3043.
[10] P. Thangadurai, V. Sabarinathan, A. Chandra Bose1, S. Ramasamy, Conductivity behavior of a cubic/tetragonal phase stabilized nanocrystalline La_2O_3-ZrO_2, Journal of Physics and Chemistry of Solids, 65(2004)1905-1912.
[11] F.I. Zhou, Y. Wang, L. Wang, Z. Cui, Z. Zhang, High temperature oxidation and insulation behavior of plasma-sprayed nanostructured thermal barrier coatings, Journal of Alloys and Compounds, 704(2017)614-623.

[12] P. Duwez, F. H. Brown, F. Odell, The zirconia-yttria system, J. of Electrochemical Society, 98(1951)356-362.
[13] X. Cao, Development of New Thermal barrier coating materials for gas turbines, 2004.
[14] A. Maricocchi, A. Barz, D. Wortman, PVD TBC experience on GE aircraft engines, thermal barrier coating workshop, NASA Lewis Research Center, Cleveland, OH, March 27-29, NASA Conference Publication, 1995, 3312, p. 79-90.
[15] C.E. Castano, M.J. O'Keefe, W.G. Fahrenholtz, Cerium-based oxide coatings, Current Opinion in Solid State and Materials Science, 19(2015)69-76.
[16] P.D.Harmsworth, R. Stevens, Microstructure and phase composition of ZrO_2-CeO_2 thermal barrier coatings, J. of Materials Science, 26(1991) 3991-3995.
[17] N.P. Padture, M. Gell, E.H. Jordan, Thermal barrier coatings for gas-turbine engine applications, Science, 296(2002)280-284.
[18] D. Zhu, J.A. Nesbitt, C.A. Barrett, T.R. McCue, and R.A. Miller, Furnace cyclic oxidation behavior of multi component low conductivity thermal barrier coatings, J. of Thermal Spray Technology, 13(2004)84-92.
[19] D. Stover, G. Pracht, H. Lehmann, M. Dietrich, J.E. Doring, and R. Vaßen, New material concepts for the next generation of plasma-sprayed thermal barrier coatings, J. of Thermal Spray Technology, 13(2004)76-83.
[20] V. Teixeira, M. Andritschky, H. Gruhn, W. Maliener, H.P. Buchkremer, D. Stoever, Failure of physically vapor deposition/plasma-sprayed thermal barrier coatings during thermal cycling, J. of Thermal Spray Technology, 9(2000)191-197.
[21] R.A. Miller, Current Status of Thermal Barrier Coatings: An overview, Surface and Coatings Technology, 30(1987)1-11.
[22] H.L. Tsai, P.C. Tsai, Microstructures and properties of laser glazed plasma sprayed ZrO_2-$YO_{1.5}$/Ni-22Cr-10Al-1 Y thermal barrier coatings, J. of Thermal Spray Technology, 4(1995)689-696.
[23] H. Chen, Y. Hao, H. Wang, W. Tang, Analysis of the microstructure and thermal shock resistance of laser glazed nanostructured zirconia TBCs, J. of Thermal Spray Technology 19(2010)558-565.
[24] X. Wang, P. Xiao, M. Schmidt, L. Li, Laser processing of yttria stabilized zirconia/alumina coatings on FeCr alloy substrates, Surface and Coatings Technology 187(2004)370-376.
[25] K. Mohammed Jasim, R.D. Rawlings, D.R.F. West, Characterization of plasma sprayed layers of fully YSZ modified by lasers, Surface Science and Technology, 53(1992)75-86.
[26] K.C. Chang, W.J. Wei, C. Chen, Oxidation behavior of thermal barrier coatings modified by laser remelting, Surface and Coatings Technology, 102(1998)197-204.
[27] B. Cortese, D. Caschera, T. de Caro, G.M. Ingo, Micro-chemical and -morphological features of heat treated plasma sprayed zirconia- based thermal barrier coatings, Thin Solid Films, 549(2013)321-329.
[28] G. Vourlias, , N. Pistofidis, P. Psyllaki, E. Pavlidou, G. Stergioudis, K. Chrissafis, Nano-phenomena during exposure of plasma-sprayed ceria stabilized zirconia 3coatings to oxygen rich environments, Journal of Alloys and Compounds, 483(2009)378–381.
[29] M. Alfano, G.D. Girolamo, L. Pagnotta, D. Sun, Processing, microstructure and mechanical properties of air plasma-sprayed ceria-yttria co-stabilized zirconia coatings, Strain, 46(2010)409-418.
[30] H. Choi, H. Kim, C. Lee, Phase evolutions of plasma sprayed ceria and yttria stabilized zirconia thermal barrier coating, J. of Materials Science Letters, 21(2002)1359-1361.
[31] Mohammed Jasim Kadhim, Mohammed Hliyil Hafiz, Maryam Abduladheem Ali Bash, Design and ٹvaluation of zirconia based thermal barrier powders for advanced engines, Engineering and Technology Jurnal, To be published 2018.
[32] J. Adams, B. Cox, The irradiation-induced phase transformation solution, J. Nuclear Engineering, Part A, 11(1959)31-33.
[33] R.A. Miller, J.L. Smaliek. G.G. Garlick, Phase stability in plasma sprayed partially stabilized zirconia-yttria, in Advances in Ceramics, Vol. 3. Edited by A.H. Heuer and L.W. Hobbs, The American Ceramic Society, Columbus, OH, 1981, pp 241-253.
[34] N. Iwamoto, N. Umesaki, Characterization of plasma sprayed zirconia coatings by X-ray diffraction and Raman spectroscopy, Thin Solid Films, 127(1985)129-137.
[35] D.L. Porter, A.H. Heuer, Microstructural development in MgO partially stabilized zirconia (Mg-PSZ), J. of the American Ceramic Society 62(1979)298-305.
[36] K. Mohammed Jasim, Laser cladding of ceramics and laser sealing of plasma sprayed zirconia based thermal barrier coatings, PhD Thesis, Royal School of Mines, Imperial College, University of London, UK, 1990.
[37] K. Mohammed Jasim, S.I. Jaffar and A.S. Hamoud, The influence of laser specific energy on laser sealing of plasma sprayed yttria partially stabilized zirconia coating, Optics and Lasers in Engineering, 51(2013)159-166.
[38] J.H. Zaat, A quarter of century of plasma spraying, Annual Review of Materials Science, 13(1983)9-42.